International Journal of Thin Films Science and Technology

http://dx.doi.org/10.12785/ijtfst/030304

Comparative Study Of CdS Thin Films Fabricated By A Simplified Spray Technique using Two Cationic Precursor Salts With Different Stability Constants

M. Anbarasi, A. R. Balu*, and V. S. Nagarethinam
PG and Research Department of Physics, AVVM Sri Pushpam College, Poondi, Thanjavur Dt, Tamilnadu, India

Email: arbalu757@gmail.com

Received: 7 Jun. 2014, Revised: 21 Aug. 2014, Accepted: 23 Aug. 2014
Published online: 1 Sep. 2014

Abstract: Cadmium sulphide (CdS) thin films were prepared by a low cost simplified spray technique using perfume atomizer on glass substrates at 325ºC using two different cationic precursors: cadmium acetate and cadmium chloride. The effect of cationic precursors on the structural, morphological, optical and electrical properties was studied. Structural studies reveal that the films are polycrystalline in nature with a mixture of both cubic and hexagonal phases with hexagonal phase being predominant irrespective of the precursor used. The preferential orientation factor f(h k l) of $CdCl_2$ based film is high compared to that of $Cd(CH_3COO)_2$ based film. Grain size value were found to be equal to 21.33 nm and 32.63 nm for $Cd(CH_3COO)_2$ and $CdCl_2$ based CdS films respectively. The optical transmittance in the visible range was found to be > 85 % for both the films. The specular reflectance values for both the films are very low. High transmittance and low reflectance values obtained for the films makes them suitable as antireflecting coating materials for thin film solar cells.

Keywords: XRD, preferential orientation, morphological studies, direct band gap, electrical properties.

1. Introduction

Cadmium sulphide is an important II-VI group chalcogenide semiconductor extensively studied in thin film form [1], nanostructures [2], etc. CdS is a direct band gap semiconductor with band gap energy of 2.42 eV at room temperature. The semiconducting behavior of CdS films arises from cadmium interstitials or from sulphur vacancies. The intermediate band gap, high absorption coefficient , low resistivity and easy ohmic contact of CdS films makes them suitable in manufacture of solar cells [3], light emitting diodes [4], photoconductors [5], sensors [6], solid state lasers and detectors [7] and optical memories [8]. CdS is known to be an excellent heterojunction partner of p-type cadmium telluride (CdTe) or p-type copper indium diselenide ($CuInSe_2$) due to its high electron affinity [9]. Also the interest in CdS thin films stems from their piezoelectric properties and potential laser applications [10]. Various synthesis techniques of fabrication of CdS thin films have been reported such as physical vapour deposition [11], thermal evaporation [12], chemical bath deposition [13], magnetron sputtering [14], molecular beam epitaxy

[15], spray pyrolysis [16] and successive ionic layer adsorption and reaction (SILAR) method [17]. Of all these techniques, physical methods of fabricating CdS thin films requires high sophisticated instrument and mismatch of thermal expansion coefficient between the film and substrate causes micro cracks, whereas chemical methods such as spray pyrolysis, chemical bath deposition, SILAR are inexpensive and are capable of producing large area coatings. Amongst the chemical methods spray pyrolysis technique is simple and easily scalable method to prepare uniform thin films over large area. However, the deposition efficiency of the spray method is relatively low because of the loss of the aerosol precursor to the surroundings which tends to reduce the low cost processing advantage, especially for the use of expensive precursors. In the present work, a simplified spray technique using perfume atomizer is employed to coat CdS thin films. The use of perfume atomizer has some specific advantages over the conventional spray technique which uses spray gun assembly: low cost, no need for carrier gas, fine atomization, improved wettability between the sprayed micro particles and loss of the precursor to the surroundings is almost nil [18]. Recently, we have reported that this simplified spray technique can be a desired alternative for the conventional spray technique by successfully fabricating CdO films [19]. Over the years, different cadmium sources have been used to prepare CdS thin films such as cadmium sulfate [20], cadmium acetate [21], cadmium iodide/nitrate and cadmium chloride [22]. Recently, Hani Khallaf et. al [23] have reported the effect of four cadmium sources on the physical properties of their chemical bath deposited CdS thin films. In this work CdS thin films were fabricated at 325ºC using cadmium acetate and cadmium chloride precursors and a comprehensive study on the effect of these precursors on the physical properties of the CdS films is performed.

2. Experimental Details

Two different cationic precursor salts cadmium acetate ($Cd(CH_3COO)_2$), 0.05M and cadmium chloride ($CdCl_2$), 0.05M were used as a source of Cd^{2+} and thiourea, 0.05M as a source of S^{2-}. Glass substrates with dimensions 76mm x 25mm x 1.4mm cleaned thoroughly with organic solvents using an ultrasonic agitator were used as substrates. CdS thin films were prepared by spraying aqueous solution (60 ml in volume) of cadmium acetate and thiourea and also by spraying aqueous solution of cadmium chloride and thiourea. The starting solution is sprayed intermittently on pre-heated substrates using a perfume atomizer. Each spray cycle has – a spray and a 2 sec wait so that the desired temperature is maintained throughout the deposition process. The film thickness was measured by means of weight gain method and compared with the values determined by employing a profilometer (Surftest SJ 301). The structural analysis was made using X-ray diffractometer (PANalytical - PW 340/60 X' Pert PRO) with CuKα radiation of wavelength 1.5406Å operated at 40 kV and 30 mA in the 2θ range 10 to 80º. AFM images were obtained using Veeco CP - II atomic force microscope. The optical transmission spectra were recorded in the 300 – 1100 nm wavelength region by using a Perkin Elmer UV-Vis-NIR double beam spectrophotometer (LAMDA- 35). The electrical parameters such as sheet

resistance (R_{sh}) and resistivity ρ were determined using d.c two point probe technique.

3. Results and Discussion

3.1 Film Formation Process

The precursor solution was atomized using perfume atomizer to form uniform stream of fine droplets. The pyrolytic decomposition of the fine droplets of Cadmium acetate and thiourea, Cadmium chloride and thiourea onto the glass substrates results in the formation of thin solid films of CdS. The possible chemical reaction that takes place is as follows:

$$Cd(CH_3COO)_2 + SC(NH_2)_2 + 2H_2O \xrightarrow{\Delta} CdS \downarrow +2CH_3COOH \uparrow +2NH_3 \uparrow +CO_2 \uparrow$$

$$CdCl_2 + SC(NH_2)_2 + 2H_2O \xrightarrow{\Delta} CdS \downarrow +2HCl + 2NH_3 \uparrow +O_2 \uparrow$$

The thickness of $Cd(CH_3COO)_2$ and $CdCl_2$ based CdS films were found to be equal to 0.243µm and 0.204µm respectively. Highest thickness was obtained in the case of Cadmium Acetate based CdS film. Similar results were obtained by Ortega-Borges et al. [24]. The low value of thickness obtained for the $CdCl_2$ based CdS film might be due to the high value of its stability constant (2.93) compared to that of $Cd(CH_3COO)_2$ which has a stability constant of 2.19. Usually the release of Cd ions from the precursor salt with high stability constant is low, which results in delayed growth mechanism of CdS and there might be excess release of unbounded sulfur ions. On the other hand for CdS films coated with cadmium acetate precursor, release of Cd^{2+} ions takes place at a rapid rate and formation of CdS with S^{2-} ions occurs at a fast rate which results in the presence of excess content of Cd which means that either interstitial Cd ions or sulfur vacancies may exist in the film, acting as donors which might be the reason for its reduced resistivity (section 3.5).

3.2 Structural Analysis

Diffractograms of CdS films prepared by the simplified spray technique using $Cd(CH_3COO)_2$ and $CdCl_2$ cationic precursors are shown in Figure. 1.

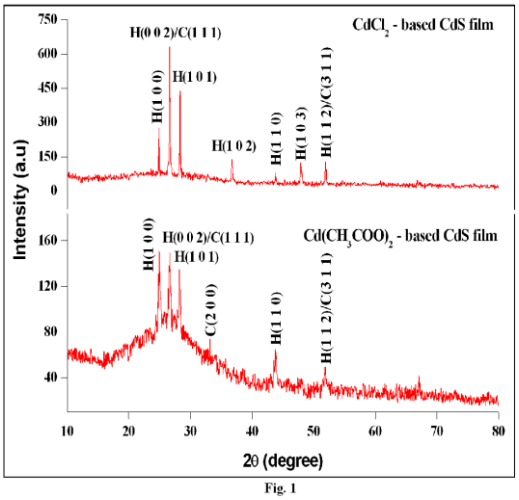

Fig. 1

Figure 1: XRD patterns of CdS films

The diffraction peaks depict that the sprayed films have a polycrystalline structure. The observed interplanar distance'd' for CdS films prepared with different Cd^{2+} source precursors is presented in Table 1 along with the standard ASTM data. It can be inferred from the observed and standard ASTM data, that CdS films obtained has a mixture of cubic and hexagonal phases. From the ASTM data for CdS, the strongest diffraction peak at 2θ = 26.63º corresponds to (0 0 2) plane for the hexagonal phase and to the (1 1 1) plane for the cubic phase.

Table 1: Comparison of observed 'd' values with standard 'd spacings (JCPDS 65 – 3414, 65 – 2887) and (h k l) planes of CdS films fabricated with different cationic precursor.

Cationic precursor	d(observed) Å	d(ASTM)		hkl planes	
		CdS (Hex)	CdS (Cubic)	CdS (Hex)	CdS (Cubic)
Cadmium Acetate	3.582	3.583	---	(1 0 0)	---
	3.359	3.357	3.360	(0 0 2)	(1 1 1)
	3.159	3.160	---	(1 0 1)	---
	2.065	2.068	---	(1 1 0)	---
	1.753	1.761	1.753	(1 1 2)	(3 1 1)
Cadmium Chloride	3.583	3.583	---	(1 0 0)	---
	3.358	3.357	3.360	(0 0 2)	(1 1 1)
	3.161	3.160	---	(1 0 1)	---
	2.065	2.068	---	(1 1 0)	---
	1.896	1.896	---	(1 0 3)	
	1.760	1.761	1.753	(1 1 2)	(3 1 1)

Table 2: Calculated preferential orientation factor f(h k l) of the CdS films

Cationic precursor	f(h k l)				
	f(1 0 0)	f(0 0 2)	f(101)	f(110)	f(112)
Cadmium Acetate	0.3037	0.3159	0.1516	0.1338	0.085
Cadmium Chloride	0.3286	0.3926	0.3391	0.1344	0.08

Table 3: Lattice and structural parameters of the CdS films

Cationic precursor	Lattice parameters				Structural parameters			
	a(Å)		c(Å)		Grain size, D (nm)	Dislocation density, δ x 10^{15} lines/m^2	Number of crystallites, N x 10^{16}	Strain, ε x 10^{-4}
	calculated	ASTM	calculated	ASTM				
Cadmium acetate	4.138	4.140	6.716	6.719	21.33	2.18	2.5	16.98
Cadmium Chloride	4.139		6.718		32.63	0.939	0.5872	5.52

The presence of hexagonal and cubic phase confirms that the deposition of CdS films in this work takes place by ion-by-ion process (heterogeneous reaction) which results in uniform compact films as evident from the AFM images (Fig. 2). Besides these, no other peaks of cubic phase CdS appeared for the films indicating that the structures of the films are predominantly hexagonal. CdS thin films in the hexagonal crystalline phase are preferred more for thin film solar cell applications due to their stability [26]. The peaks at 2θ = 24.96º, 28.29º, 43.81º, and 47.94º corresponds to (1 0 0), (1 0 1), (1 1 0), and (1 0 3) planes [JCPDS 65 – 3414, 65 – 2887]. The preferred orientation factor f(h k l) of the peaks ((1 0 0), (0 0 2), (1 0 1), (1 1 0) and (1 1 2)) of the CdS films were calculated and given in Table 2. It is observed that the value of f(0 0 2) is large irrespective of the cationic precursor used when compared with f(h k l) of other peaks indicating a strong orientational growth along the (0 0 2) plane. The value of f(0 0 2) of $CdCl_2$ based CdS film is high compared to that of $Cd(CH_3COO)_2$ based CdS film indicating better crystallinity. The predominance of (0 0 2) plane in the films clearly showed that the growth of the crystal is such that the c-axis is perpendicular to the surface of the substrate and this growth pattern is not affected by the source of the cationic precursors.

The lattice parameters, 'a' and 'c' of the unit cell was evaluated according to the relation [27]:

$$\frac{1}{d^2} = \frac{4}{3}\frac{h^2 + hk + k^2}{a^2} + \frac{l^2}{c^2} \qquad (1)$$

and the calculated lattice parameter values are given in Table 3.

The structural parameters such as grain size (D), dislocation density (δ), number of crystallites per unit area (N) and strain (ε) were determined using the formulae [28 – 30]:

$$D = \frac{0.94\lambda}{\beta \cos\theta} \qquad (2)$$

$$\delta = \frac{1}{D^2} \qquad (3)$$

$$N = \frac{t}{D^3} \quad (4)$$

$$\varepsilon = \frac{\beta \cos\theta}{4} \quad (5)$$

The lattice parameters of the CdS films prepared using different cationic precursors by the simplified spray technique are well agreed with the ASTM values and it is observed that the cationic sources has no significant influence on the lattice parameter values. The smaller values of strain and dislocation density obtained for $CdCl_2$ based CdS films confirms the good crystallinity of the films fabricated with that precursor salt.

3.3 Surface Morphological Studies

The AFM images of the CdS films are shown in Figure. 2. For chemically deposited chalcogenide thin films, the grain size and configuration is mainly influenced by many parameters such as composition and temperature of the solution, nature of the substrate, etc. In this work, the grain size is predominantly influenced only by the cationic precursor used. The 2D and 3D AFM images of $Cd(CH_3COO)_2$ based CdS film (Figure. 2(a, b)) depicts island growth on the film.

The calculated structural parameters are presented in Table 3.

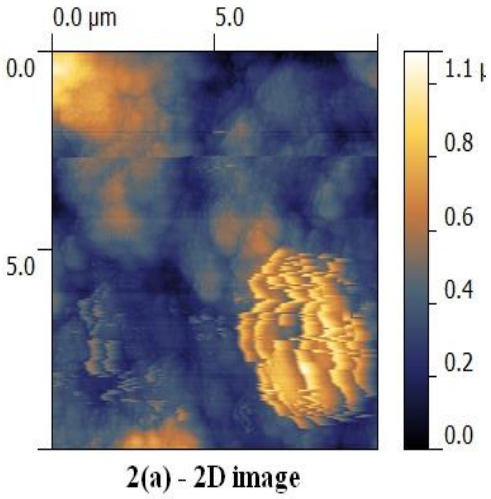

2(a) - 2D image

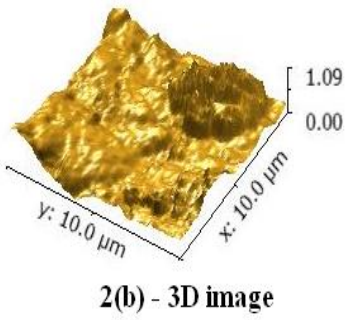

2(b) - 3D image

Figure 2(a, b): AFM images of cadmium acetate based CdS film

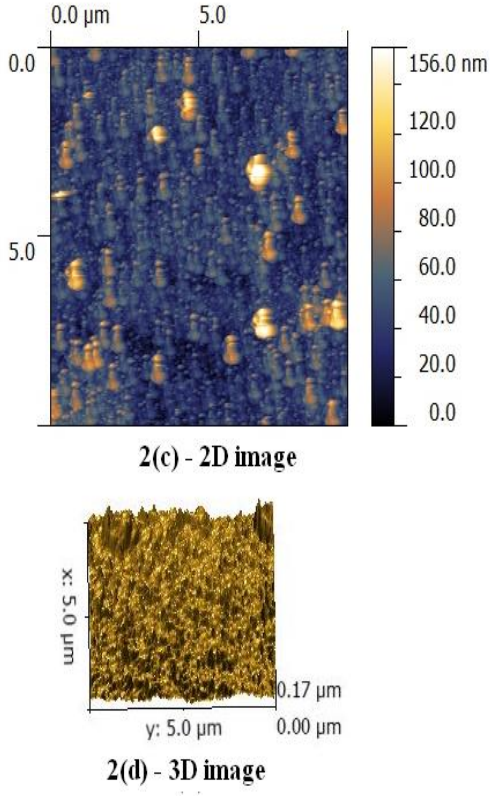

Figure 2 (c, d): AFM images of cadmium chloride based CdS film

This island formation is attributed to rapid nucleation and crystal growth of CdS due to a large number of free cadmium metal ions which is the characteristic nature of the precursor salt with low stability constant. Figure. 2(c, d) showed the AFM images of $CdCl_2$ based CdS film. The films surface appears to be smooth and densely packed with CdS grains, which resulted from the slow release of cadmium metal ions. Thus in this work the precursor salt alone influences the morphology of CdS films fabricated by this simplified spray technique.

3.4 UV-Vis_NIR Spectroscopy Studies

Study of materials by means of optical absorption provides a simple method for explaining some features concerning the band structure of materials. Optical absorption measurements of CdS films were carried out in the wavelength range 300 – 1100 nm. Figure. 3 shows the variation of absorbance with wavelength of CdS films fabricated using different cationic precursors.

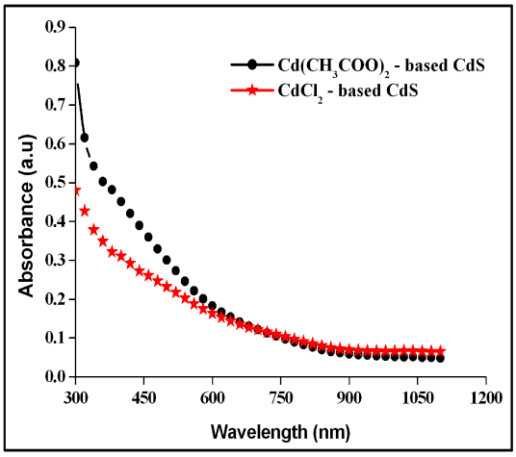

Figure 3: Variation of absorbance with wavelength of CdS films

The spectra show two regions, one for higher wavelength (> 700 nm) showing practically low absorption and other for lower wavelength (< 600 nm) in which absorption increases rapidly for both the samples. In the lower wavelength region the absorption of $CdCl_2$ based CdS film is less than that of $Cd(CH_3COO)_2$ based CdS film which might be the reason for the high percentage transmittance value obtained for that film in this region (Figure. 6). The above discussion holds good for the high absorption value obtained in $Cd(CH_3COO)_2$ based CdS film in the wavelength region (> 700 nm).

The optical absorption coefficient (α) can be deduced from the absorption spectra using the relation

$$\alpha = \frac{2.303A}{t} \qquad (6)$$

where t is the thickness of the as deposited CdS films. The optical band gap E_g was determined by analysing the optical data with the expression for the absorption coefficient (α) and the photon energy (hγ) using Tauc formula for direct band gap semiconductor [31]:

$$(\alpha h\gamma)^2 = A(h\gamma - E_g) \qquad (7)$$

where A is a constant which depends on the transition probability, E_g is the optical gap energy, γ is the frequency of the incident photon and h is the Planck's constant. The energy band gap was estimated from the straight line of the plot $(\alpha h\gamma)^2$ versus photon energy for CdS thin films as shown in Figure. 4. Extrapolation of linear portion of the graph to the energy axis at α = 0 gives the band gap energy of the CdS films.

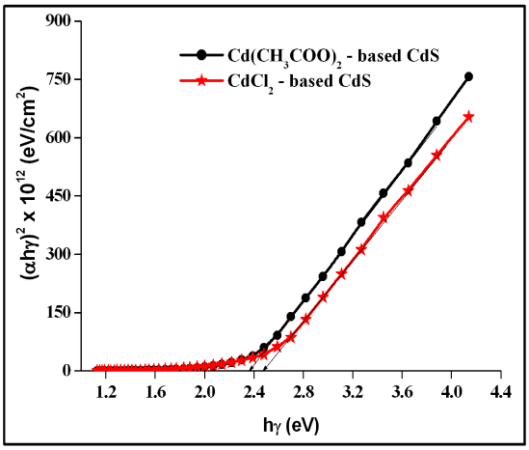

Figure 4: Variation of $(\alpha h\gamma)^2$ versus hγ of the CdS films

The values of E_g for $Cd(CH_3COO)_2$ and $CdCl_2$ based CdS films were found to be equal to 2.36 eV and 2.48 eV respectively. The calculated films' band gaps are in good agreement with the reported values [32]. The value of E_g for $Cd(CH_3COO)_2$ based CdS film is less than that for $CdCl_2$ based CdS film which may be due to the presence of impurity electronic levels in the forbidden gap of $Cd(CH_3COO)_2$ based CdS film.

Tauc has identified three distinct regions in the absorption spectrum of amorphous semiconductors: a) the weak-absorption tail which originates from defects and impurities, b) the exponential edge region which is strongly related to the structural randomness of the glassy material, and c) the high absorption edge region which determines the optical energy gap. In the exponential edge region the absorption coefficient α(hγ) is well described by the exponential law

$$\alpha = \alpha_0 \exp\left(\frac{h\gamma}{E_u}\right) \qquad (8)$$

known as Urbach law [33]. Here α_0 is a constant, hγ is the incident photon energy, and E_u is called Urbach energy, which characterizes the slope of the exponential edge region and is width of the band tails of the localized states. The formation of localized states with energies at the boundaries of the energy gap is one of the effects of the structural disorder on the electronic structure of amorphous materials. This is the reason why the Urbach energy is frequently used as a measure of the degree of structural disorder. E_u is given by the relation:

$$E_u = \left[\frac{d(\ln(\alpha))}{d(h\gamma)}\right]^{-1} \qquad (9)$$

The graph of ln(α) versus hγ being the photon energy is given in Figure. 5.

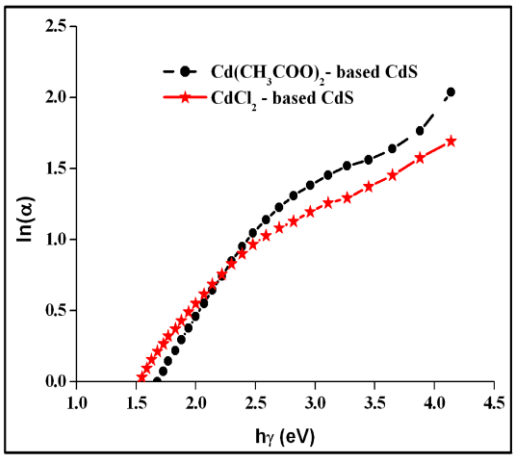

Figure 5: The graph of ln(α) versus hγ of the CdS films

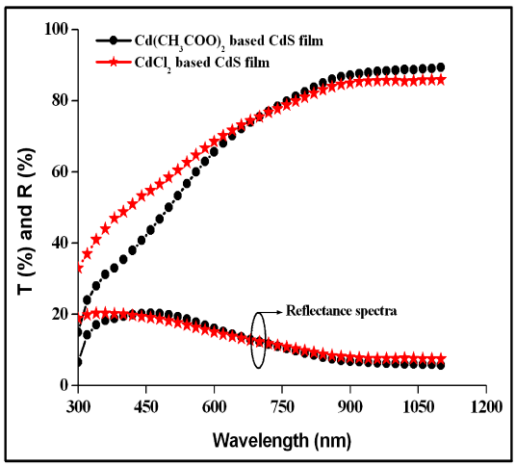

Figure 6: Variation of T % and R % with wavelength of the CdS films

The values of E_u for $Cd(CH_3COO)_2$ and $CdCl_2$ based CdS films were found to be equal to 1.124 meV and 0.35 meV respectively. The value of E_u for $Cd(CH_3COO)_2$ based CdS film is high indicating that there is deviation of its bond length and angle from the standard value. Since optical band gap value is governed by the disorder variation, an increase in the band tail width causes the reduction in the optical gap value obtained for $Cd(CH_3COO)_2$ based CdS film. Low value of E_u obtained for $CdCl_2$ based CdS film suggests that there is reduction in the disorder of the film and as a result its E_g value is increased.

The optical transmittance and reflectance spectra of the CdS films are shown in Figure. 6.

For both the precursors, films showed good transmission (> 85%) for wavelengths larger than 600 nm, and this property is one of the prerequisites for solar cell window layers. High transmittance values obtained for both the films imply that the films has a lower defect density and thus in turn may have better electrical properties because absorption of light in the longer wavelength region (> 600 nm) is usually caused by crystalline defects such as grain boundaries and dislocations [34]. The transmission of $Cd(CH_3COO)_2$ based CdS film is slightly higher than that of $CdCl_2$ based CdS film. Usually CdS films with higher thickness have low transmission. But in this work, the percentage transmittance of $Cd(CH_3COO)_2$ based CdS film is high, compared to $CdCl_2$ based CdS film even though the thickness of the former is greater than the later. This might be due to the reduced resistivity value obtained for the $Cd(CH_3COO)_2$ based CdS film. The transmittance of CdS thin films is expected to depend on three factors: a) oxygen deficiency, b) surface roughness (surface scattering reduces the transmission, which in turn depends on the grain size and shape) and c) impurity centers. The reduction of

the transparency of $CdCl_2$ based CdS film in the wavelength range (750 – 1200 nm) may originate from the light scattering on the film surface due to film surface coverage by overgrown crystallites which results in the surface roughness of $CdCl_2$ based CdS films. These observations are strongly supported from the AFM images, which showed that $CdCl_2$ based film is much smoother and more uniform than $Cd(CH_3COO)_2$ based film. The overall specular reflectance for the CdS films coated with $Cd(CH_3COO)_2$ and $CdCl_2$ precursors is very low. The high transmittance and low reflectance values obtained for the films makes them suitable as antireflecting coating materials for thin film solar cells.

Refractive index is one of the fundamental properties for an optical material because it is closely related to the electronic polarization of ions and the local field inside materials. The complex optical constant (refractive index, (n)) of the as-deposited CdS films has been evaluated by the relation [35]:

$$n = \frac{1+R}{1-R} \pm \sqrt{\frac{4R}{(1-R)^2} - k^2} \qquad (10)$$

where $k = \frac{\alpha\lambda}{4\pi}$ is the extinction coefficient.

The variation of refractive index and extinction coefficient of the CdS films are shown in Figures. 7 and 8 respectively.

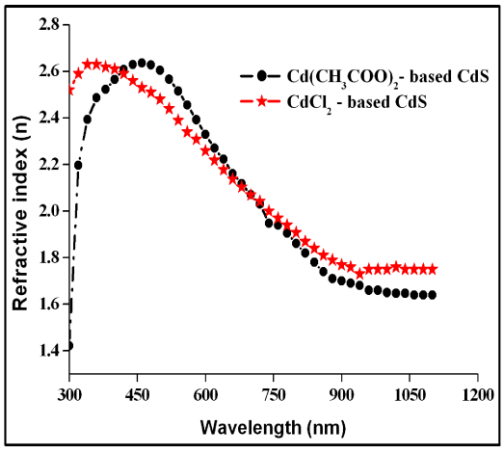

Figure 7: Variation of refractive index with wavelength of CdS films fabricated with different cationic precursors

From Figure 7 it is observed that up to 450 nm, the refractive index increases with wavelength for both the films. The refractive index decreases with increasing wavelength from 450 nm – 920 nm which indicates that the present CdS films show a normal dispersion. In the near IR region, the value of n remains constant for both the films. The value of n was found to be equal to 1.64 and 1.75 for $Cd(CH_3COO)_2$ and $CdCl_2$ based CdS films respectively. The high value of n obtained for $CdCl_2$ based CdS films can be attributed to an increase of its surface roughness which acts to decrease the effective mean free path through increased surface scattering [36] and this fact strongly favours the reason for the reduction of its transparency.

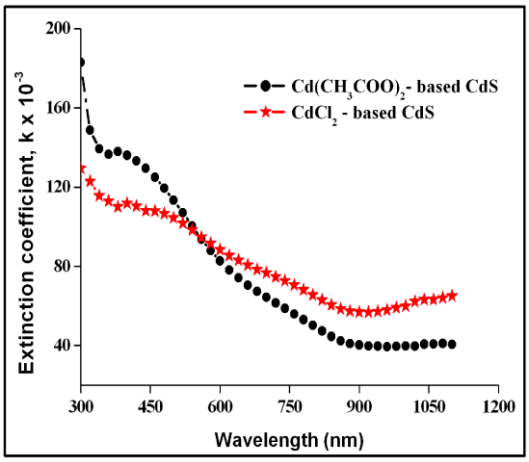

Figure 8: Variation of extinction coefficient with wavelength of the CdS films

The source k (absorption) refers to the inelastic scattering of the electromagnetic waves in the semiconductor such as the Compton effect, photoelectric effect, pair production effect and so on [37]. The variation in the extinction coefficient (Figure. 8) is paralleled by the absorbance of films, the high value of k obtained for the CdS films upto 450 nm indicates a high absorption in this wavelength region which might be the reason for the reduced transmittance values obtained for the CdS films in this region. The optical constants (n, k) of the CdS films have an inverse relation with the transmittance spectrum. The high (low) transmittance spectra have low (high) optical constants.

From the refractive index data, the packing density which is defined as the ratio of the solid volume to the total volume of the film is estimated using the relation [38]:

$$n_f = n_s p + (1 - p)\, n_v \qquad (11)$$

where n_f is the refractive index of the film, n_s is the refractive index of the bulk material and n_v is the refractive index of voids, which are generally filled with ambient, i.e. air. The calculated packing density values of $Cd(CH_3COO)_2$ and $CdCl_2$ based CdS films were found to be equal to 2.133 and 2.5 respectively. The high value of packing density obtained for $CdCl_2$ based CdS film indicates its good crystallinity.

Refractive index dispersion plays an important role particularly in designing optical devices. The dispersion parameters of the as-deposited CdS films were calculated to analyze their choice in designing optical devices. According to the Wemple-DiDomenico single oscillator model, the refractive index (n) of a dielectric medium in the region of low absorption is given by [39].

$$\left(n^2 - 1\right)^{-1} = \frac{E_o}{E_d} - \frac{1}{E_o E_d}\left(h\gamma\right)^2 \qquad (12)$$

where n is the refractive index, h is the Planck's constant, γ is the frequency, hγ is the photon energy, E_o is the average excitation energy for electronic transitions (single oscillator energy) and E_d is the dispersion energy parameter, which is a measure of the strength of an interband optical transition. From the $(n^2\text{-}1)^{-1}$ versus $(h\gamma)^2$ graph (Figure. 9), E_d and E_o can be directly determined from the slope $(E_dE_o)^{-1}$ and intercept E_o/E_d at the vertical axis.

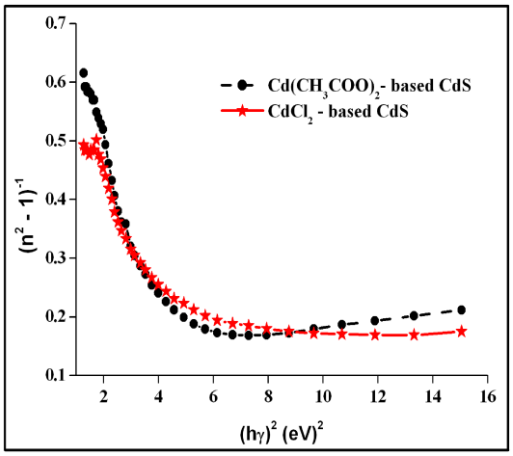

Figure 9: $(n^2 -1)^{-1}$ versus $(h\gamma)^2$ graph of CdS films

The obtained values of E_o and E_d are presented in Table 4. The obtained values of E_o and E_d suggest that the single-oscillator model is valid for the coated CdS films. A measure of interband transition strengths can be provided from the M_{-1} and M_{-3} moments of the optical spectrum. The M_{-1} and M_{-3} moments are expressed as [40]:

$$M_{-1} = \frac{E_d}{E_o},$$

$$M_{-3} = \frac{E_d}{E_o^3} \qquad (13)$$

The calculated values of M_{-1} and M_{-3} are given in Table 4.

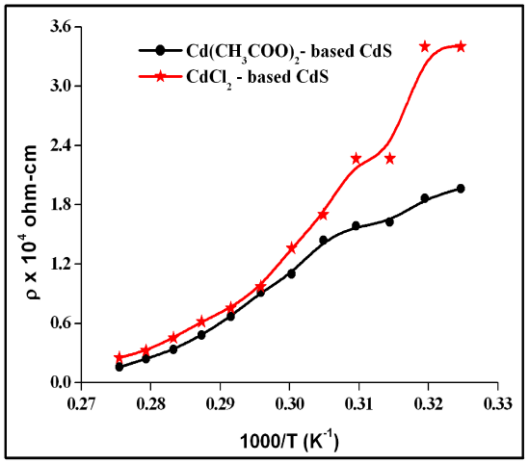

Figure 10: Variation of resistivity with reciprocal of temperature of the CdS films

Table 4: Single oscillator parameters of the CdS films

Cationic precursor	E_g (eV)	E_o (eV)	E_d (eV)	E_o/E_d	M_{-1}	M_{-3} $(eV)^{-2}$
$Cd(CH_3COO)_2$	2.36	2.39	14.94	0.16	6.25	1.094
$CdCl_2$	2.48	2.79	13.28	0.21	4.94	0.611

3.5 Electrical Studies

The resistivity of the as-deposited CdS films was determined by the two point probe method using aluminium strips and their values were calculated using the relation,

$$\rho = \frac{R \times A}{L} \qquad (14)$$

where R is the resistance given by the slope of the V-I characteristic curves, A is the coated area of the film under investigation and L is the spacing between the strips. Figure. 10 shows the variation of resistivity of CdS films with reciprocal of temperature. For both the films, the resistivity decreases with increase in temperature indicating semiconducting nature of the films. The measured resistivity of the CdS films coated with $Cd(CH_3COO)_2$ and $CdCl_2$ precursors were found to be equal to 0.8613×10^1 ohm-cm and 1.481×10^1 ohm-cm respectively. The resistivity values obtained are found to be comparable with the value obtained for CdS thin films prepared using $CdSO_4$ precursor by Khallaf et al.[23]. In their work they obtained a resistivity in the order of 10^2 ohm-cm and 10^3 ohm-cm for CdS thin films fabricated using cadmium acetate and cadmium chloride precursors by CBD technique. The low value of resistivity obtained for $Cd(CH_3COO)_2$ based CdS film might be due to its high mobility and carrier concentration compared to that of $CdCl_2$ based CdS thin film. For both the films, resistivity follows the relation:

$$\rho = \rho_o \exp(E_a / kT) \qquad (15)$$

from which the activation energy E_a of the CdS films required for conduction is calculated. The activation energies for the CdS films with $Cd(CH_3COO)_2$ and $CdCl_2$ precursors were found to be equal to 0.25 eV and 0.24 eV respectively. The calculated values of activation energies of the as deposited CdS films are in good agreement with the reported value [41]. The values of activation energy for the CdS films fabricated with different precursors are almost the same i.e. the required energy for conduction for both the films are the same.

4. Conclusion

Structural, surface morphological, optical and electrical properties of the CdS films fabricated at 325ºC by a simplified spray technique using cadmium acetate and cadmium chloride precursors have been studied in detail. The structural studies revealed that the films have preferential orientation along the (0 0 2) plane for the hexagonal phase irrespective of the cationic precursors used. The lattice parameter values (a = 4.139Å and c= 6.718Å) of $CdCl_2$ based CdS film agrees well with ASTM data. The smaller values of strain and dislocation density obtained for $CdCl_2$ based CdS film confirms the better crystallinity of the film fabricated with that precursor. The low value of Urbach energy obtained for $CdCl_2$ based CdS film suggests that there is reduction in the disorder of the film coated with this precursor. The resistivity value for $Cd(CH_3COO)_2$ based CdS film is low which might be due to its high mobility and carrier concentration. Thus with thiourea as a source for sulphur ions, $Cd(CH_3COO)_2$ based CdS film have better properties such as high transmittance and low resistivity compared to that of $CdCl_2$ based film. But regarding good crystallinity, surface smoothness and structural parameters, $CdCl_2$ precursor is better than cadmium acetate precursor especially for solar cell and other optical device applications.

Acknowledgements

The authors are grateful to the Secretary and Correspondent, AVVM Sri Pushpam College (Autonomous), Poondi for his excellent encouragement and support.

References

[1] D.S. Chuu, C.M. Dai, Phys.Rev.B. 45, 11805 (1992).

[2] F.R. Oulton, V.J. Sorger, T. Zengraf, R.M. Ma, C. Gladden, L. Dai, G. Bartal, X. Zhang, Nature. 461, 629 (2009).

[3] H. Metin, R. Esen, Semicond.Sci.Technol.18, 175 (2003).

[4] J.L. Zhao, J.A. Bardecker, A.M. Munro, M.S. Liu,Y.H. Niu, I.K. Ding, J.D. Luo, B.Q. Chen, A.K.Y. Jen, D.S. Ginger, Nano Lett. 6, 463 (2006).

[5] J.R. Maltby, C.E. Reed, C.G. Scott, Surf. Sci. 51, 89 (1975).

[6] C. Li, D. Zhang, X. Liu, S. Han,T.ang, J. Han, C. Zhou, Appl.Phys.Lett. 82, 1613 (2003).

[7] P.C. Rieke, S.B. Bentjen, Chem.Mater. 5, 43 (1993).

[8] Y. Fainman, J. Ma, S.H. Lee, Mater. Sci. Rep. 9, 53 (1993).

[9] K.D. Dobson, I. Visoly-Fisher, G. Hodes, D. Cahen, Solar Energy Materials and Solar cells, 62, 295 (2000).

[10] J. Lee, Appl.Surf. Sci. 252, 1398 (2005).

[11] J.H. Lee, W.C. Song, J.S. Yi, K.J. Yang, W.D. Han, J. Hwang, Thin Solid Films, 431, 349 (2003).

[12] S.A. Mahmoud, A.A. Ibrahim, A.S. Riad, Thin Solid Films, 372, 144 (2000).

[13] A.I. Oliva, O. Solis–Canto, R. Castro-Rodriguez, P. Quintana, Thin Solid Films, 391, 28 (2001).

[14] S. Bonilla, E.A. Dalchiele, Thin Solid Films, 204, 397 (1991).

[15] K.B. Ozanyan, J.E. Nicholls, L. May, J.H.C. Hogg, W.E. Hagstan, B. Lunn, D.E.Ashenford, Solid State Commun. 99, 407 (1996).

[16] V.S. Nagarethinam, N. Arunkumar, A.R. Balu, M. Suganya, G. Selvan, J. Electron Devices, 14, 1108 (2012).

[17] X.X. Liu, Z.G. Jin, S.J. Bu, J. Zhao, Z.J. Cheng, J. Inorg. Mater. 19, 691 (2004).

[18] T. Fukano, T. Motohiro, Solar Energy Mater. Solar cells, 82, 567 (2004).

[19] K. Usharani, A.R. Balu, G. Shanmugavel, M. Suganya, V.S. Nagarethinam, Int. J. Sci. Res. Rev. 2, 53 (2013).

[20] H. Metin, R. Esen, Semicond. Sci. Technol. 18, 647 (2003).

[21] M. Anbarasi, T. Sivaraman, V.S. Nagarethinam, A.R. Balu, Int. J. Chem. Phys. Sci. 3, 1 (2014).

[22] T. Nakanishi, K. Ito, Sol. Energy. Mater. Sol. Cells, 35, 171 (1994).

[23] H. Khallaf, O. Oladeji Isaiah, Guangyu Chai, Lee Chow, Thin Solid Films, 516, 7306 (2008).

[24] R. Ortega–Borges, D. Lincot, J.Electrochem .Soc.140, 3464 (1993).

[25] H. Metin, S. Erat, F.M. Emen, V. Kafadar, A.N. Yazini, M. Ari, N. Kulcu, Journal of Luminescence. 130, 1531 (2010).

[26] T. Sivaraman, V.S. Nagarethinam, A.R. Balu, Res. J. Mater. Sci. 2, 6 (2014).

[27] N. Manjula, K. Usharani, A.R. Balu, V.S. Nagarethinam, Int. J. Chemtech. Research. 6, 705 (2014).

[28] A.R. Balu, V.S. Nagarethinam, M.G. Syed Basheer Ahamed, A. Thayumanavan, K.R. Murali, C. Sanjeeviraja, V. Swaminathan and M. Jayachandran, *Materials Sci. Eng*., 171, 93 (2010).

[29] A.R. Balu, V.S. Nagarethinam, M. Suganya, N. Arunkumar, G.Selvan, J. Electron Devices, 12, 739 (2012).

[30] S. Prabahar, M. Dhanam, J.Cryst. Growth. 285, 41 (2005).

[31] J. Tauc, Amorphous and Liquid semiconductors, Plenum Press, NewYork, (1976).

[32] B. Su, K.L. Choy, Thin Solid Films 361, 102 (2000).

[33] F. Urbach, Phys. Rev. 92, 1324 (1953).

[34] J. Hiie, T. Dedova, V. Valdna, K. Muska, Thin Solid Films, 443, 511 (2006).

[35] C. Rajashree, A.R. Balu, V.S. Nagarethinam, Int. J. Chemtech. Research. 6, 347 (2014).

[36] A. Bendavid, P.J. Martin, L. Wieczorek, Thin Solid Films, 354, 169 (1999).

[37] H. Czichos, T. Saito, L. Smith, Handbook of materials measurement methods, Springer, Leipzig, (2006).

[38] K.P. Mohanachandra, H.G. Shanbhouge and J. Uchil, Phys. Status. Solidi. A, 130, 45 (1992).

[39] F. Yakuphanoglu, A. Cukurovali and I. Yilmaz, Physica B, 353, 210 (2004).

[40] M. DiDomenico, S.H. Wemple, Phys. Rev. B 3, 1338 (1971).

[41] C.D. Gutierrez Lazos, E. Rosendo, M. Ortega, A.I. Oliva, O. Tapia, T. Diaz, H. Juarez, G. Garcia, M. Rubin, Mater. Sci. Engineering: B. 65, 74 (2009).